Understanding brain complexity in naturalistic processing in humans

Lucy L. W. Owen[1], and Jeremy R. Manning[1,†]

[1]Department of Psychological and Brain Sciences,
Dartmouth College, Hanover, NH
[†]Address correspondence to jeremy.r.manning@dartmouth.edu

February 13, 2023

Abstract

We applied dimensionality reduction algorithms to the activity patterns in each experimental condition. Specifically, we sought to understand the "dimensionality" of the neural patterns that were sufficient to decode participants' listening times (or approach was similar to that of Mack et al. 2017). We found that even low-dimensional embeddings of the data were sufficient to accurately decode listening times from the intact story recording, whereas finer temporal scramblings of the story required higher-dimensional embeddings of the data to reach peak decoding accuracy.

Introduction

We're interested in the complexity of brain patterns that underly different types of thoughts. To explore this question space, we take brain patterns recorded under different experimental conditions and project them into lower dimensional spaces using principle components analysis. We can then ask how well those low-dimensional embeddings of the data retain cognitively relevant information like when in a story someone is listening to. Then we can explore decoding accuracy as a function of the number of components, or dimensions, in the low-dimensional space under different cognitive conditions.

You can imagine two reasonable predictions of how cognition is reflected in brain patterns. The first is as our thoughts become more complex, they are supported by more complex brain patterns, and require more components to decode. The second is that when thoughts are deeper and more complicated, the units of neural activity would carry more information, and would require therefore fewer components to decode.

This idea can be explored in this visual analogy (Fig. **??**) for neural compression. Here there are two images of pies, the top pie is more complex than the bottom. On the left we're illustrating that it takes fewer componenets to reach the same 95 percent variance explained in the less complex pie, which corresponds to higher compression. However, on the right with very few components similar variance is explaining both pies.

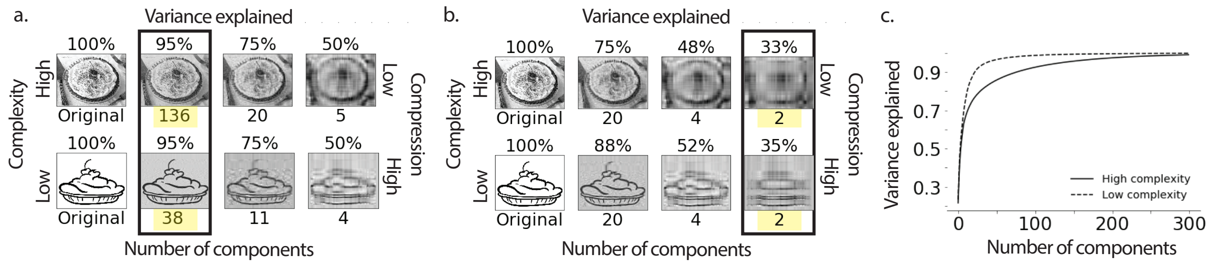

Figure 1: **Illustration of compression.** Visual analogy for neural compression. Here are 2 images of pies, one more complex thantheother. **a.**It takes fewer components to reach the same percent variance explained in the less complex pie, which corresponds to higher compression. **b.**However, with very few components, similar variance is explained in both pies. **c.** Plots the cumulative explained variance for more and more components.

We investigated the dimensionality of neural patterns by training classifiers using more and more principle components. Or, in other words, we used less and less compression to decode. We applied the approach to a neuroimaging dataset comprising data collected as participants listened to a story varying in cognitive richness (**?**).

Methods

Dimensionality reduction

Explain PCA

Evaluation metrics

We evaluated the degree of compression of held-out neuroimaging data with the time at which it was collected. We used this latter evaluations (using timepoint decoding) as a proxy for gauging how much explanatory power the compressed data held with respect to the observed data.

Timepoint decoding

To explore how higher-order structure varies with stimulus structure and complexity, we used a previous neuroimaging dataset **?** in which participants listened to an audio recording of a story; 36 particpants listen to an intact version of the story, 17 participants listen to time-scrambled recordings of the same story where paragraphs were scrambled, 36 particpants listen to word-scrambled version and 36 participants lay in rest condition.

Prior work has shown participants share similar neural responses to richly structured stimuli when compared to stimuli with less structure. To assess whether the moment-by-moment higher order correlations were reliably preserved across participants, we used inter-subject functional connectivity (ISFC) to isolate the time-varying correlational structure (functional connectivity patterns that were specifically driven by the story participants listened to. Following the analyses conducted by (HTFA) **?**, we first applied *hierarchical topographic factor analysis* (HTFA) to the fMRI datasets to obtain a time series of 700 node activities for every participant. We then applied dimensionality reduction (Incremental PCA) for each group.

We then compared the groups' activity patterns (using Pearson correlations) to estimate the story times each corresponding pattern using more and more principle components.

To assess decoding accuracy, we randomly divided participants for each stimulus into training and testing groups. We then compared the groups' activity patterns (using Pearson correlations) to estimate the story times each corresponding pattern using more and more principle components (as the data became less compressed). Specifically, we asked, for each timepoint: what are the correlations between the first group's and second group's activity patterns at each order. We note that the decoding test we used is a conservative in which we count a timepoint label as incorrect if it is not an exact match.

Results

For our decoding analysis, we used HTFA-derived node activities **?** from fMRI data collected as participants listened to an audio recording of a story (intact condition; 36 participants), listened to time scrambled recordings of the same story (17 participants in the paragraph-scrambled condition listened to the paragraphs in a randomized order and 36 in the word-scrambled condition listened to the words in a randomized order), or lay resting with their eyes open in the scanner (rest condition; 36 participants). We sought to understand the 'dimensionality' of the neural patterns by using more and more principle components to decode a multi-subject fMRI datasets. This story listening dataset was collected as part of a separate study, where the full imaging parameters, image preprocessing methods, and experimental details may be found (**?**). The dataset is available at http://arks. princeton.edu/ark:/88435/dsp015d86p269k.

We performed a decoding analysis, using cross validation to estimate (using other participants' data) which parts of the story the additional added principle component corresponded to (see *Materials and methods*). We note that our primary goal was not to achieve perfect decoding accuracy, but rather to use decoding accuracy as a benchmark for assessing whether different neural features specifically capture cognitively relevant brain patterns.

Separately for each experimental condition, we divided participants into two groups. Starting with 1 principle comonent, for each dimension we added another principle component, and we correlated the

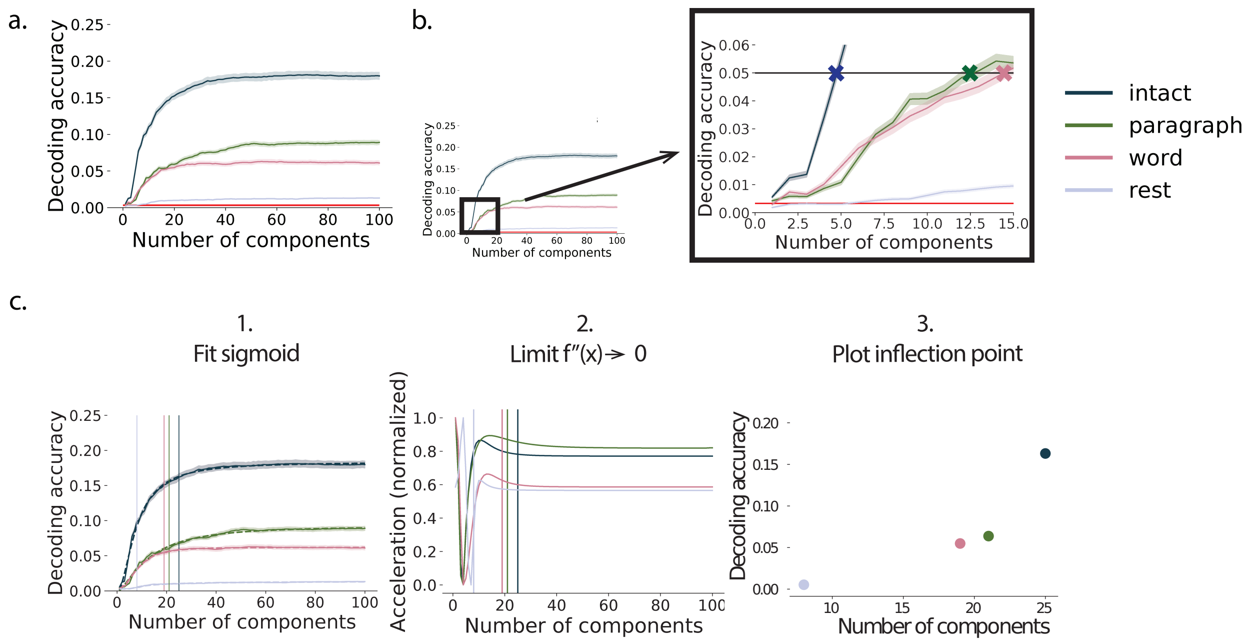

Figure 2: **Decoding accuracy. a. Decoding accuracy by number of components.** Ribbons of each color display cross-validated decoding performance for each condition (intact, paragraph, word, and rest). Decoders were trained using increasingly more principle components and displayed relative to chance (red line). **b. Fixed decoding accuracy by number of components.** We zoom in on the plot shown in **a.** and add a line denoting fixed decoding accuracy (.05). We plot where the intact, paragraph, and word conditions intersect. **c. Explanation of inflection metric.** First the we fit a sigmoid function to the decoding accuracy by number of components. Second, we found where the second derivate is both positive and less than .0001. Last, we then plot that inflection point as a single metric to capture the slope and asymptote of the curve.

group 1 activity patterns with group 2 activity patterns. There were 272 timepoints for paragraph condition, 300 timepoints for intact and word conditions, and 400 timepoints for rest condition, so chance performance on this decoding test is was $\frac{1}{272}$, $\frac{1}{300}$, and $\frac{1}{400}$ respectively.

- As complexity of the stimulus increases, decoding accuracy increases (Fig. 2, a.). Replication of Simony findings.

- As complexity of the stimuli increases, we need fewer components to decode the same amount (Fig. 2, b.).

- As complexity of the stimuli increases, more components are required to reach peak decoding accuracy (Fig. 2, c.).

As complexity of the stimuli increases, decoding accuracy increases with higher cognitive areas. (Fig. **??**).

If, there is some understanding of the narrative that accumulates over time, we should be able to see that change.

- Increases in decoding accuracy with the same number or fewer components for more complex, cognitively rich, conditions. - Decreases in decoding accuracy for the word-scrambled and rest condition.

Discussion

- We trained classifiers using more and more principle components to decode, and compared across conditions with varying degrees of cognitive richness. -We found that as listening conditions become more cognitively rich, decoding accuracy increased. -Also, decoding accuracy increased as understanding of the narrative accumulated over time, in more complex listening conditions. - Decoding accuracy also increased in higher cognitive areas, in more complex listening conditions. -We found that as story listening conditions become more complex, more components are required to decode. -We also found we could decode better with more impoverished data when there is the underlying structure of the narrative providing more cognitive richness. -We posit that as the complexity of our thoughts increases, neural compression decreases. However, as our thoughts become deeper and richer, more reliable information is available at higher neural compression.

Based on prior work (**?**) and following the direction of the field (**?**) we think our thoughts might be encoded in dynamic network patterns, and possibly higher order network patterns (Fig. **??**). We sought to test this hypothesis by developing an approach to inferring high-order network dynamics from timeseries data.

One challenge in studying dynamic interactions is the computational resources required to calculate higher-order correlations. We developed a computationally tractable model of network dynamics (Fig. **??**)

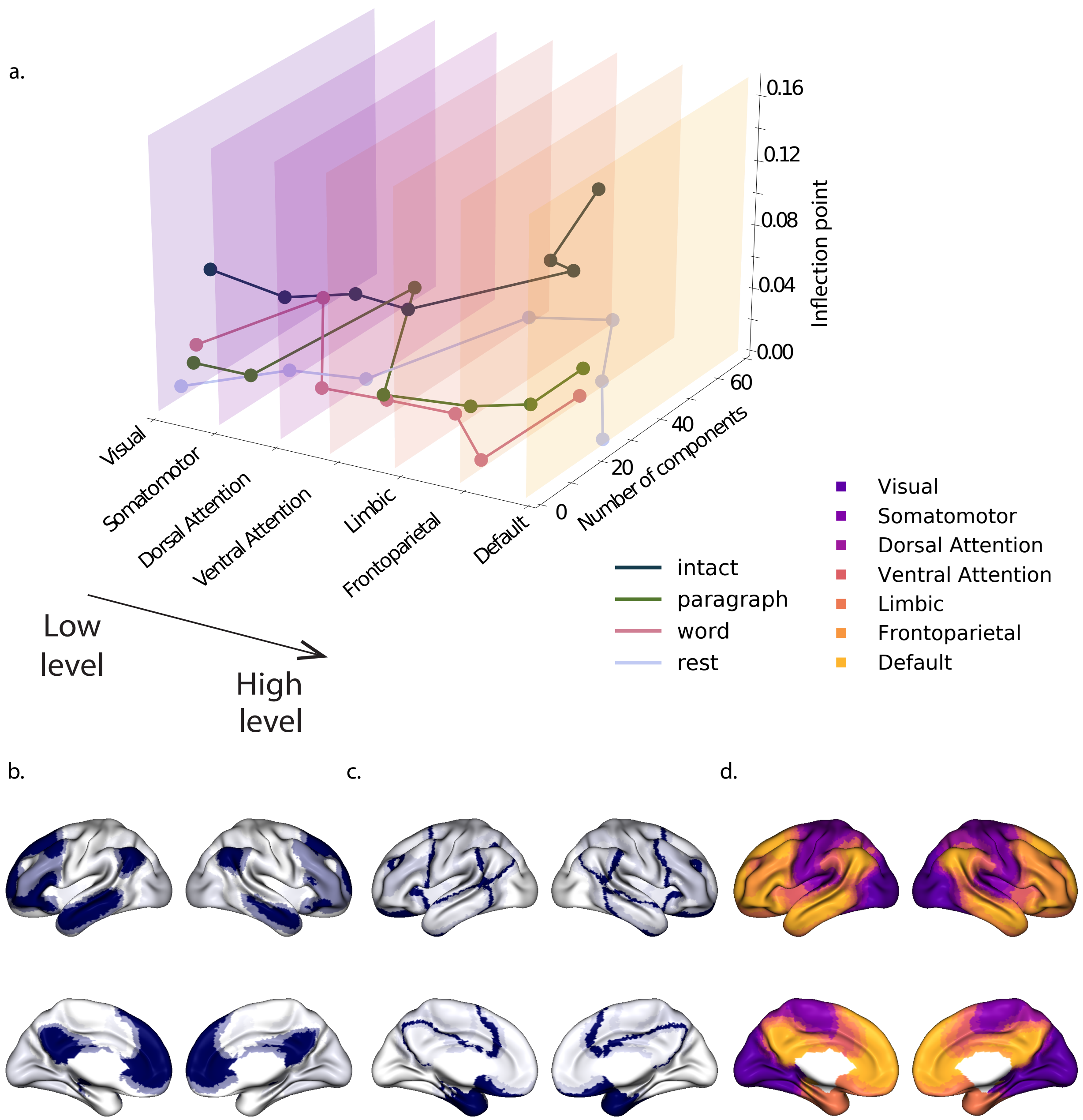

Figure 3: **Inflection points by network. a.** Inflection point was calculated as explained in Fig. 2, b. Analyses were limited by the brain networks (using the Yeoetal11 network parcellation) and arranged in increasing order relative to the intact condition. **b. and c.** For the total time in the intact condition, we are plotting the relative inflection points (**b.**) and corresponding number of components (**c.**) by network. **d.** The network parcellation defined by Yeo et al. (2011) is displayed on the inflated brain maps. The colors and network labels serve as a legend for **a.** and **d.**

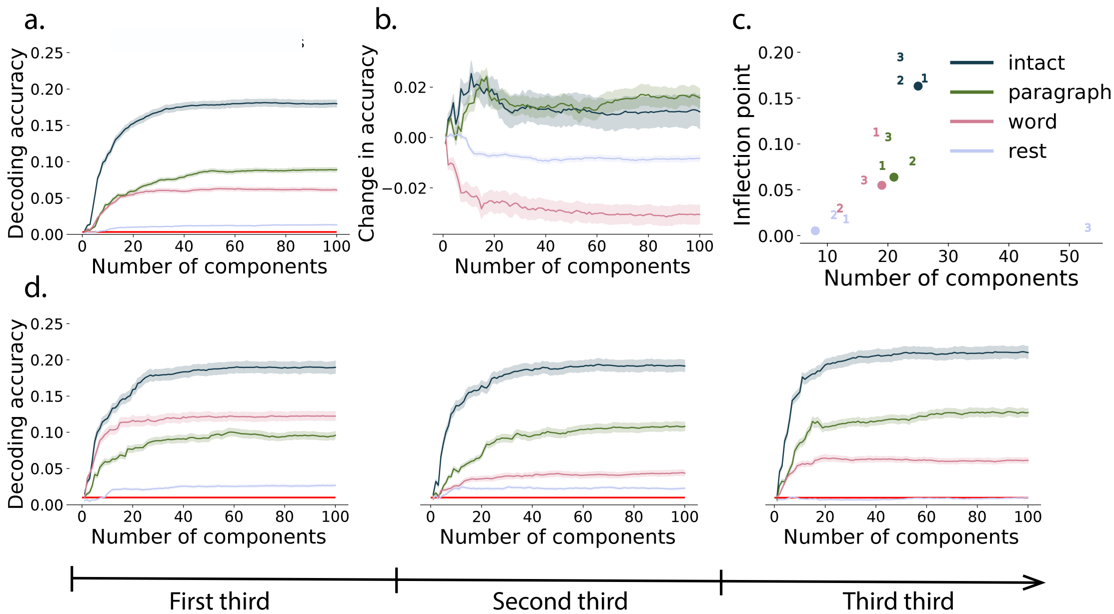

Figure 4: **Inflection points by thirds.** **a.** Decoding accuracy by number of components not broken into thirds (Fig. 2 a.). **b. and c.** Quantifying changes in decoding accuracy across time. **b.** Slope of decoding accuracy was calculated by fitting a regression line for each component/condition for each third. **c.** We also repeated the analysis (Fig. 2, b.) to obtain the inflection point for each condition and for each third. **d.** Decoding accuracy by number of components for each third of the scan time. We repeated the same analysis in Fig. 2 a. but breaking the scan time for each condition into 3 intervals.

that takes in a feature timeseries and outputs approximated first-order dynamics (i.e., dynamic functional correlations), second-order dynamics (reflecting homologous networks that dynamically form and disperse), and higher-order network dynamics (up to tenth-order dynamic correlations).

We first validated our model using synthetic data, and explored how recovery varied with different underlying data structures and kernels. We then applied the approach to an fMRI dataset (**?**) in which participants listened to an audio recording of a story, as well as scrambled versions of the same story (where the scrambling was applied at different temporal scales). We trained classifiers to take the output of the model and decode the timepoint in the story (or scrambled story) that the participants were listening to. We found that, during the intact listening condition in the experiment, classifiers that incorporated higher-order correlations yielded consistently higher accuracy than classifiers trained only on lower-order patterns (Fig. **??**, a.&d.). By contrast, these higher-order correlations were not necessary to support decoding the other listening conditions and (minimally above chance) during a control rest condition. This suggests that the cognitive processing that supported the most cogntively rich listening conditions involved second-order (or higher) network dynamics.

Although we found decoding accuracy was best when incorporating higher-order network dynamics for all but rest condition, it is unclear if this is a product of the brain or the data collection technique. It could be that the brain is second-order or it could be that fMRI can only reliably give second-order interactions. Exploring this method with other data collection technique will be important to disentangle this question.

Concluding remarks

How can we better understand how brain patterns change over time? How can we quantify the potential network dynamics that might be driving these changes? One way to judge the techniques of the future is to look at the trajectory of the fMRI field so far has taken so far (Fig. **??**). The field started with univariate activation, measuring the average activity for each voxel. Analyses of multivariate activation followed, looking at spatial patterns of activity over voxels. Next, correlations of activity were explored, first with measures like resting connectivity that take temporal correlation between a seed voxel and all other voxels then with full connectivty that measure all pairwise correlations. Additionally, this path of increasing complexity also moved from static to dynamic measurements. One logical next step in this trajectory would be dynamic higher-order correlations. We have created a method to support these calculations by scalably approximating dynamic higher-order correlations.

Acknowledgements

We acknowledge discussions with Luke Chang, Hany Farid, Paxton Fitzpatrick, Andrew Heusser, Eshin Jolly, Qiang Liu, Matthijs van der Meer, Judith Mildner, Gina Notaro, Stephen Satterthwaite, Emily Whitaker, Weizhen Xie, and Kirsten Ziman. Our work was supported in part by NSF EPSCoR Award Number 1632738 to J.R.M. and by a sub-award of DARPA RAM Cooperative Agreement N66001-14-2-4-032 to J.R.M. The content is solely the responsibility of the authors and does not necessarily represent the official views of our supporting organizations.

Author contributions

Concept: J.R.M. Implementation: T.H.C., L.L.W.O., and J.R.M. Analyses: L.L.W.O and J.R.M.

References